Math. & Comput. Sci., 7(1) 2026, 118–137

Online: ISSN 2717-2708

Mathematics and Computational Sciences

Journal Homepage: http://mcs.qut.ac.ir/mcs

An innovative Bernoulli operational matrix framework for regularized Prabhakar fractional optimal control problems

Chaima Boutiba[a,b], Ahmed Bokhari[a,b,*], Rachid Belgacem[a,b], Dumitru Baleanu[c,d]

[a] *Faculty of Exact Sciences and Computer Science, Hassiba Benbouali University of Chlef, Algeria.*

[b] *Laboratory of Mathematics and its Applications LMA, Hassiba Benbouali University of Chlef, Algeria.*

[c] *Department of Computer Science and Mathematics, Lebanese American University, Beirut, Lebanon.*

[d] *Institute of Space Sciences, Magurele-Bucharest, Romania.*

Abstract

This paper introduces a novel operational matrix approach for addressing a class of fractional-order optimal control problems, where the derivative is taken in the regularized Prabhakar sense. The method employs Bernoulli polynomials and utilizes their operational matrix of regularized Prabhakar derivative and inherent properties to convert the original problem into a finite-dimensional optimization problem. Using the Lagrange multiplier approach, the required optimality conditions are derived, yielding an algebraic system from the original problem. Solving this system yields an approximate fractional optimal solution. The practicality and efficiency of the proposed approach are confirmed via a series of numerical examples.

Keywords: Fractional optimal control problems, Regularized Prabhakar derivative, Operational matrix, Lagrange multipliers.

2020 MSC: 26A33, 49Mxx, 65K05.

1. Introduction

Optimal control problems constitute a significant class of infinite-dimensional optimization problems in which the objective is to find a control function that minimizes (or maximizes) a performance index, subject to dynamic constraints typically formulated as differential equations. These problems naturally arise in a wide range of disciplines, including engineering, economics, biology, and physics. A notable subclass is the linear-quadratic control problem, characterized by linear system dynamics and a performance index quadratic in both the state and control variables. This type of problem has broad applications across various domains such as aeronautics [14], robotics [22], economics [42], and engineering [5, 12]. In recent years, fractional optimal control problems have attracted growing attention due to their ability to model systems with memory and hereditary properties. In this context, the classical differential operator in the dynamic equations is replaced by a fractional operatorsuch as the Caputo [4, 3], RiemannLiouville [2, 1], CaputoFabrizio [13, 44], or AtanganaBaleanu operator [41]which enables a more accurate representation of complex phenomena with long-term memory effects. These formulations are particularly

*Corresponding author

Email addresses: c.bouthiba@univ-chlef.dz (Chaima Boutiba), a.bokhari@univ-chlef.dz (Ahmed Bokhari), belgacemrachid02@yahoo.fr (Rachid Belgacem), dumitru.baleanu@lau.edu.lb (Dumitru Baleanu)

doi: 10.30511/mcs.2026.2067782.1426

Received: 03 August 2025 Accepted: 02 January 2026

relevant in applications including viscoelastic materials [6, 25], battery dynamics [36, 21], anomalous diffusion [26, 27], and biological systems [18, 24]. In this study, we focus on the regularized Prabhakar operator, a generalization of the Caputo and RiemannLiouville operators that offers greater flexibility for modeling such systems. Optimal control problems are typically approached using one of two main strategies: analytical or numerical methods. The analytical approachrelying on indirect methods such as Pontryagins Minimum Principle or Bellmans Dynamic Programmingcan yield exact solutions. However, in practice, solving the resulting differential systems is often highly complex or even intractable. As a result, numerical methods are widely adopted, offering approximate solutions with satisfactory accuracy.

Among these, operational matrix methods stand out for their ability to convert differential or integral operators into matrix products. This transformation reduces the problem to a finite-dimensional optimization problem. These matrices are typically constructed from families of basis functions or polynomials. Such techniques have been successfully applied to both classical and fractional control problems, using bases like Legendre polynomials [35, 23, 29], Boubaker polynomials [32, 33], Genocchi polynomials [39, 40], Bernoulli polynomials [20, 34, 11] and B-spline functions [38].

In this work, we introduce a novel approach to solving a class of linear-quadratic optimal control problems using an operational matrix constructed from Bernoulli polynomials. Specifically, we develop this matrix for the regularized Prabhakar operator, which generalizes both Caputo and RiemannLiouville operators. By leveraging the product matrix and key properties of Bernoulli polynomials, the original problem is reduced to a finite-dimensional optimization problem. The resulting algebraic system can then be solved efficiently, either through direct solvers or by applying the method of Lagrange multipliers. Several numerical examples are provided to validate the efficiency and practicality of the proposed method.

To the best of our knowledge, this is the first work addressing the approximate solution of optimal control problems involving the regularized Prabhakar operator. To further validate our approach, we compare it with solutions obtained using the Caputo operatora special case of the regularized Prabhakar operator when $\xi = 0$.

The paper is structured as follows: Section 2 provides a review of key concepts in fractional calculus and Bernoulli polynomials. Section 3 presents the derivation of the regularized Prabhakar operational matrix and its corresponding product matrix. Section 4 presents the error analysis and discusses convergence results. In Section 5, the considered optimal control problem is presented, along with a detailed outline of the method used to compute an approximate solution. Section 6 showcases several numerical examples that illustrate the accuracy and effectiveness of the proposed approach. Finally, concluding remarks are offered in the last section.

2. Preliminaries

For clarity, the following paragraphs present essential preliminaries, including key definitions, fundamental concepts, and important properties of the Prabhakar fractional operator.

Definition 2.1. The left-sided Riemann-Liouville fractional integral $({}^{RL}I^{\mu}_{0+})$ of a given function $\mathscr{W}$ of order $(\mu > 0)$ is defined as [37]:

$$ {}^{RL}I^{\mu}_{0+}\mathscr{W}(t) = \frac{1}{\Gamma(\mu)}\int_0^t \frac{\mathscr{W}(\tau)}{(t-\tau)^{1-\mu}}d\tau, \quad t > 0. \tag{2.1}$$

Definition 2.2. The left-sided Caputo fractional derivative $({}^{C}D^{\mu}_{0+})$ of order $(\mu > 0)$ for a sufficiently smooth function $(\mathscr{W})$ is defined as [8]:

$$ {}^{C}D^{\mu}_{0+}\mathscr{W}(t) = \begin{cases} \dfrac{1}{\Gamma(p-\mu)}\displaystyle\int_0^t (t-\tau)^{p-\mu-1}\mathscr{W}^{(p)}(\tau)\,d\tau, & \text{if } p-1 < \mu < p, \\ \dfrac{d^p}{dt^p}\mathscr{W}(t), & \text{if } \mu = p, \end{cases} $$

where $p = \lceil \mu \rceil \in \mathbb{N}$ and $\Gamma(\cdot)$ is the Gamma function.

Definition 2.3. The 1-parameter MittagLeffler function is defined by [15]

$$E_\sigma(\omega) = \sum_{r=0}^{\infty} \frac{\omega^r}{\Gamma(\sigma r + 1)}, \quad \omega, \sigma \in \mathbb{C},\ Re(\sigma) > 0 \tag{2.2}$$

The 2- parameter MittagLeffler function reads [43]

$$E_{\sigma,\mu}(\omega) = \sum_{r=0}^{\infty} \frac{\omega^r}{\Gamma(\sigma r + \mu)},\ \omega, \sigma, \mu \in \mathbb{C}, Re(\sigma) > 0 \tag{2.3}$$

Note that $E_{\sigma,1}(\omega) = E_\sigma(\omega)$.

A variant of the Mittag-Leffler function involving three parameters is denoted by $E^{\xi}_{\sigma,\mu}(\omega)$ and is defined as follows [31, 10]:

$$E^{\xi}_{\sigma,\mu}(\omega) = \sum_{r=0}^{\infty} \frac{1}{\Gamma(\xi)} \frac{\Gamma(\xi + r)}{\Gamma(\sigma r + \mu)} \frac{\omega^r}{r!}, \omega, \sigma, \mu, \xi \in \mathbb{C},\ \ Re(\sigma) > 0. \tag{2.4}$$

In practical applications, a further generalization of Eq. (2.4) is often employed, given by:

$$e^{\xi}_{\sigma,\mu,\omega}(t, \omega) = t^{\mu-1} E^{\xi}_{\sigma,\mu}(\omega t^\sigma), \tag{2.5}$$

Definition 2.4. [31] Let $\mathscr{W} \in L^1[0, b]$ with $0 < t < b \leqslant \infty$. The Prabhakar integral operator is defined as

$$\mathbf{E}^{\xi}_{\sigma,\mu,\omega,0^+}\mathscr{W}(t) = \int_0^t (t-\tau)^{\mu-1} E^{\xi}_{\sigma,\mu}(\omega(t-\tau)^\sigma)\mathscr{W}(\tau)\, d\tau = \left(\mathscr{W} * e^{\xi}_{\sigma,\mu,\omega}\right)(t), \tag{2.6}$$

where σ, μ, ξ, ω are complex parameters, and $\Re(\sigma), \Re(\mu) > 0$.

Theorem 2.5. *[19] Let* $\sigma, \mu, \xi, \upsilon, \omega \in \mathbb{C}(\Re(\sigma), \Re(\mu), \Re(\upsilon) > 0)$, *then*

$$\int_0^t (t-\tau)^{\mu-1} E^{\xi}_{\sigma,\mu}[\omega(t-\tau)^\sigma] \tau^{\upsilon-1} d\tau = \Gamma(\upsilon)\, t^{\mu+\upsilon-1} E^{\xi}_{\sigma,\mu+\upsilon}(\omega t^\sigma).$$

It is worth recalling that the Prabhakar derivative serves as the left-inverse of the integral operator defined in Eq. (2.7).

Definition 2.6. [31] Let $\mathscr{W} \in L^1[0, b]$, with $0 < t < b \leqslant \infty$, and assume that $\mathscr{W} * e^{-\xi}_{\sigma,p-\mu,\omega}(\cdot) \in W^{p,1}[0, b]$, where $p = \lceil \mu \rceil$ is the smallest integer greater than or equal to μ. The Prabhakar fractional derivative is then defined by:

$$\mathbf{D}^{\xi}_{\sigma,\mu,\omega,0^+}\mathscr{W}(t) = \frac{d^p}{dt^p}\left[\mathbf{E}^{-\xi}_{\sigma,p-\mu,\omega,0^+}\mathscr{W}(t)\right], \tag{2.7}$$

where σ, μ, ξ, ω are complex parameters and $\Re(\sigma) > 0$, $\Re(\mu) > 0$.

The classical RiemannLiouville fractional integral of order $p - (\mu + \theta)$ is a particular case of the Prabhakar integral operator when $\xi = 0$ [17].

$$I^{p-(\mu+\theta)}_{0^+}\mathscr{W}(t) = \mathbb{E}^{0}_{\sigma,p-(\mu+\theta),\omega,0^+}\mathscr{W}(t), \tag{2.8}$$

where $\sigma, \mu, \theta, \omega \in \mathbb{C}$ are the parameters of the Prabhakar kernel, and $p = \lceil \mu + \theta \rceil$ ensures that the fractional order is properly defined.

Note that the operator $\mathbf{E}^{0}_{\sigma,p-(\mu+\theta),\omega,0^+}$ is convergent under the conditions $\sigma > 0$, $p - (\mu + \theta) > 0$, $\mathscr{W} \in L^1[0, T]$, and $|\omega| t^\sigma < 1$. By applying equation (2.8), the Prabhakar fractional derivative $\mathbb{D}^{\{\sigma,\mu,\omega,0^+\},\xi}\mathscr{W}(t)$ can be expressed as follows [9]:

$$\mathbf{D}^{\xi}_{\sigma,\mu,\omega,0^+}\mathscr{W}(t) = \frac{d^p}{dt^p}\left[\mathbf{E}^{-\xi}_{\sigma,p-\mu,\omega,0^+}\mathscr{W}(t)\right], \tag{2.9}$$

where $D^{\mu+\theta}_{0^+}$ denotes the RiemannLiouville fractional derivative of order $\mu + \theta$.

Definition 2.7. [16] Let $\mathscr{W} \in AC[0,b], 0 < t < b \leqslant \infty$, and $p = \lceil \mu \rceil$. The regularized Prabhakar's derivative is defined by

$$ {}^{C}\mathbf{D}^{\xi}_{\sigma,\mu,\omega,0^+}\mathscr{W}(t) = \int_{0^+}^{t} (t-\tau)^{p-\mu-1} E^{-\xi}_{\sigma,p-\mu}\big(\omega(t-\tau)^{\sigma}\big)\mathscr{W}^{(p)}(\tau)\, d\tau. \tag{2.10} $$

where $\sigma, \mu, \xi, \omega \in \mathbb{C}$, $\Re(\sigma), \Re(\mu) > 0$.

Remark 2.8. [17] If $\xi = 0$, the regularized Prabhakar derivative becomes the Caputo fractional derivative.

Remark 2.9. [30] Let $\mathscr{W} \in AC^{p}(0,b)$, with $0 < t < b \leqslant \infty$ and $\mu > 0$. Then:

$$ {}^{C}\mathbf{D}^{\xi}_{\sigma,\mu,\omega,0^+}\mathscr{W}(t) = \mathbf{D}^{\xi}_{\sigma,\mu,\omega,0^+}\left(\mathscr{W}(t) - \sum_{k=0}^{p-1}\frac{t^k}{k!}\mathscr{W}^{(k)}(0^+)\right). $$

This result illustrates the link between the standard and regularized versions of the Prabhakar derivative. In particular, when certain parameters vanish, the regularized form coincides with the classical Caputo derivative, as also shown by Garra et al., who introduced the regularized Prabhakar operator and discussed its properties.

Theorem 2.10. *[28] Let* $\sigma, \mu, \xi > 0$, $n \in \mathbb{N}$. *Then:*

$$ \mathbf{E}^{\xi}_{\sigma,\mu,\omega,0^+} t^{n} = \frac{n!}{\Gamma(\xi)} \sum_{r=0}^{\infty} \frac{\Gamma(\xi+r)\,\omega^{r}\, t^{\sigma r+\mu+n}}{r!\,\Gamma(\sigma r+\mu+n+1)}. \tag{2.11} $$

Proof. Let us consider the function $\mathscr{W}(t) = t^{n}$. By applying Definition 2.4 together with Theorem 2.5, we obtain

$$ \mathbf{E}^{\xi}_{\sigma,\mu,\omega,0^+} t^{n} = \int_{0}^{t} (t-\tau)^{\mu-1} E^{\xi}_{\sigma,\mu}\big(\omega(t-\tau)^{\sigma}\big)\tau^{n}\, d\tau = \Gamma(n+1)\, t^{\mu+n}\, E^{\xi}_{\sigma,\mu+n+1}\big(\omega t^{\sigma}\big). $$

Then, using relation (2.4), we directly arrive at the desired result (2.11), which completes the proof. □

Theorem 2.11. *Let* $\sigma, \mu, \xi > 0$ *and let* $s \in \mathbb{N}$. *Then*

$$ {}^{C}\mathbf{D}^{\xi}_{\sigma,\mu,\omega,0^+} t^{q} = \begin{cases} 0, & \text{if } q < \lceil \mu \rceil, \\ \displaystyle\sum_{j=0}^{\infty} \frac{q!\,\Gamma(-\xi+j)\,\omega^{j}\, t^{j\sigma+q-\mu}}{\Gamma(-\xi)\,\Gamma(\sigma j+q-\mu+1)\,j!}, & \text{if } q \geqslant \lceil \mu \rceil. \end{cases} $$

where $\lceil \cdot \rceil$ *denotes the ceiling function.*

Proof. We recall that for a real number q and an integer j, the following holds:

$$ \frac{d^{j}}{dt^{j}} t^{q} = \begin{cases} 0, & \text{if } q < j, \\ \dfrac{q!}{(q-j)!}\, t^{q-j}, & \text{if } q \geqslant j. \end{cases} $$

Let $p = \lceil \mu \rceil$. According to Definition 2.7, for $q < p$, the regularized Prabhakar derivative vanishes:

$$ {}^{C}\mathbf{D}^{\xi}_{\sigma,\mu,\omega,0^+} t^{q} = 0. $$

For $q \geqslant p$, we have:

$$ {}^{C}\mathbf{D}^{\xi}_{\sigma,\mu,\omega,0^+} t^{q} = \mathbf{E}^{-\xi}_{\sigma,p-\mu,\omega,0^+}\left(\frac{d^{p}}{dt^{p}} t^{q}\right) = \frac{q!}{(q-p)!}\mathbf{E}^{-\xi}_{\sigma,p-\mu,\omega,0^+} t^{q-p}. $$

Applying the integral definition of the Prabhakar operator, we obtain:

$$\begin{aligned}
{}^{C}\mathbf{D}^{\xi}_{\sigma,\mu,\omega,0^+} t^q &= \frac{q!}{(q-p)!}\int_0^t (t-\tau)^{p-\mu-1} E^{-\xi}_{\sigma,p-\mu}\left(\omega(t-\tau)^{\sigma}\right)\tau^{q-p}\,d\tau \\
&= \frac{q!}{(q-p)!}\Gamma(q-p+1)\,t^{q-\mu}E^{-\xi}_{\sigma,q-\mu+1}(\omega t^{\sigma}) \\
&= \sum_{j=0}^{\infty}\frac{q!\,\Gamma(-\xi+j)\,\omega^j\,t^{j\sigma+q-\mu}}{\Gamma(-\xi)\,\Gamma(\sigma j+q-\mu+1)\,j!}.
\end{aligned}$$

This result follows directly from Theorem 2.5, and completes the proof. □

2.1. Bernoulli Polynomials

The classical Bernoulli polynomials $\mathscr{B}_N(t)$ are defined through the exponential generating function

$$\frac{xe^{xt}}{e^x-1} = \sum_{N=0}^{\infty}\mathscr{B}_N(t)\frac{x^N}{N!}.$$

In particular, the Bernoulli numbers correspond to the evaluation of these polynomials at zero: $\mathscr{B}_N = \mathscr{B}_N(0)$.

An explicit expression for the Bernoulli polynomial of degree N on the interval $[0,1]$ is given by

$$\mathscr{B}_N(t) = \sum_{r=0}^{N}\binom{N}{r}\mathscr{B}_{N-r}\,t^r = \sum_{r=0}^{N}\binom{N}{r}\mathscr{B}_r\,t^{N-r}.$$

Some fundamental properties of the Bernoulli polynomials include:

$$\mathscr{B}'_N(t) = N\,\mathscr{B}_{N-1}(t), \qquad N \geqslant 1, \tag{2.12}$$

$$\mathscr{B}_N(1-t) = (-1)^N\,\mathscr{B}_N(t), \tag{2.13}$$

$$\mathscr{B}_N(0) = \mathscr{B}_N, \qquad \mathscr{B}_N(1) = (-1)^N\mathscr{B}_N, \tag{2.14}$$

$$\int_0^1 \mathscr{B}_N(t)\,dt = 0, \qquad \text{for } N \geqslant 1. \tag{2.15}$$

2.2. Function Approximation

Any function $\mathscr{W}(t)$, squareintegrable over the interval $[0,1]$, can be represented approximately as

$$\mathscr{W}(t) \approx \sum_{r=0}^{N} c_r\,\mathscr{B}_r(t),$$

where the coefficients c_r are given by

$$c_r = \langle \mathscr{W}(t), \mathscr{B}_r(t)\rangle H^{-1},$$

where $H \in \mathbb{R}^{(N+1)\times(N+1)}$ is the Gram matrix defined by

$$H(t) = \langle \mathscr{B}(t), \mathscr{B}(t)\rangle = \int_0^1 \mathscr{B}(t)\,\mathscr{B}^T(t)\,dt. \tag{2.16}$$

Let $c = [c_0, c_1, \ldots, c_N]$ and $\mathscr{B}(t) = [\mathscr{B}_0(t), \mathscr{B}_1(t), \ldots, \mathscr{B}_N(t)]^T$. Then

$$\mathscr{W}(t) \approx \mathbf{c}\,\mathscr{B}(t), \qquad \mathbf{c} = H^{-1}\langle f(t), \mathscr{B}(t)\rangle.$$

3. Bernoulli Operational Matrix of the Regularized Prabhakar Derivative

In this section, we present a unified and original framework for constructing an operational matrix for the Regularized Prabhakar fractional derivative based on the Bernoulli polynomial basis. The objective is to express the action of this nonlocal operator in matrix form, thereby converting the underlying fractional differential system into an equivalent algebraic system.

This construction offers a novel and efficient numerical tool for addressing fractional optimal control problems involving Prabhakar-type dynamics. The use of Bernoulli polynomials provides a compact representation with computational advantages, making the proposed scheme both accurate and suitable for handling the memory-dependent behavior inherent in fractional models.

Theorem 3.1. *Let* $\mathscr{B}(t) = [\mathscr{B}_0(t), \mathscr{B}_1(t), \dots, \mathscr{B}_N(t)]^T$ *denote the vector of Bernoulli polynomials, and let* $0 < \sigma < 1$. *Then the regularized Prabhakar fractional derivative in the Caputo sense of order* σ *satisfies:*

$$D^{\xi}_{\sigma,\mu,\omega}\mathscr{B}(t) = P^{\xi}_{\sigma,\mu,\omega}\mathscr{B}(t),$$

where $P^{\xi}_{\sigma,\mu,\omega} \in \mathbb{R}^{(N+1)\times(N+1)}$ *is the operational matrix defined by:*

$$P^{\xi}_{\sigma,\mu,\omega}(j,l) = \begin{cases} 0, & \text{for } 0 \leqslant j < \lceil \mu \rceil, \\ \displaystyle\sum_{i=\lceil \mu \rceil}^{j} \zeta^{\xi}_{j,i,\sigma,\mu,\omega,l}, & \text{for } j \geqslant \lceil \mu \rceil, \end{cases}$$

with the coefficients $\zeta^{\xi}_{j,i,\sigma,\mu,\omega,l}$ *given by:*

$$\zeta^{\xi}_{j,i,\sigma,\mu,\omega,l} = \binom{j}{i} \mathscr{B}_{j-i} \sum_{k=0}^{\infty} \frac{\Gamma(-\xi+k)\omega^k \Gamma(i+1) g_l^{(k,i)}}{\Gamma(-\xi)\Gamma(\sigma k - \mu + i + 1)\Gamma(k+1)},$$

and where $g_l^{(k,i)}$ *are the coefficients obtained by projecting* $t^{\sigma k-\mu+i}$ *onto the Bernoulli basis:*

$$t^{\sigma k-\mu+i} \approx \sum_{l=0}^{N} g_l^{(k,i)} \mathscr{B}_l(t), \quad \text{with} \quad g_l^{(k,i)} = \sum_{m=0}^{N} \left(H^{-1}\right)_{l,m} \left\langle t^{\sigma k-\mu+i}, \mathscr{B}_m(t) \right\rangle,$$

where $H \in \mathbb{R}^{(N+1)\times(N+1)}$ *is computed according to* (2.16).

To clearly illustrate the structure of the matrix $P^{\xi}_{\sigma,\mu,\omega} \in \mathbb{R}^{(N+1)\times(N+1)}$, we present its entries explicitly by separating the cases $j < \lceil \mu \rceil$ and $j \geqslant \lceil \mu \rceil$ as follows:

$$P^{\xi}_{\sigma,\mu,\omega} = \begin{bmatrix} 0 & 0 & \cdots & 0 \\ \vdots & \vdots & \ddots & \vdots \\ 0 & 0 & \cdots & 0 \\ \displaystyle\sum_{i=\lceil \mu \rceil}^{\lceil \mu \rceil} \zeta^{\xi}_{\lceil \mu \rceil,i,\sigma,\mu,\omega,0} & \cdots & \cdots & \displaystyle\sum_{i=\lceil \mu \rceil}^{\lceil \mu \rceil} \zeta^{\xi}_{\lceil \mu \rceil,i,\sigma,\mu,\omega,N} \\ \displaystyle\sum_{i=\lceil \mu \rceil}^{\lceil \mu \rceil+1} \zeta^{\xi}_{\lceil \mu \rceil+1,i,\sigma,\mu,\omega,0} & \cdots & \cdots & \displaystyle\sum_{i=\lceil \mu \rceil}^{\lceil \mu \rceil+1} \zeta^{\xi}_{\lceil \mu \rceil+1,i,\sigma,\mu,\omega,N} \\ \vdots & & \ddots & \vdots \\ \displaystyle\sum_{i=\lceil \mu \rceil}^{N} \zeta^{\xi}_{N,i,\sigma,\mu,\omega,0} & \cdots & \cdots & \displaystyle\sum_{i=\lceil \mu \rceil}^{N} \zeta^{\xi}_{N,i,\sigma,\mu,\omega,N} \end{bmatrix}.$$

To highlight the sparse and structured nature of the matrix $P^{\xi}_{\sigma,\mu,\omega}$, we express it in block form as follows:

$$P^{\xi}_{\sigma,\mu,\omega} = \begin{bmatrix} \mathbf{0}_{\lceil\mu\rceil\times(N+1)} \\ \widetilde{P}^{\xi}_{\sigma,\mu,\omega} \end{bmatrix},$$

where $\widetilde{P}^{\xi}_{\sigma,\mu,\omega} \in \mathbb{R}^{(N+1-\lceil\mu\rceil)\times(N+1)}$ is defined by

$$\left(\widetilde{P}^{\xi}_{\sigma,\mu,\omega}\right)_{j,l} = \sum_{i=\lceil\mu\rceil}^{j+\lceil\mu\rceil} \zeta^{\xi}_{j+\lceil\mu\rceil,i,\sigma,\mu,\omega,l}.$$

Proof. We begin with the classical expansion of the Bernoulli polynomial $\mathscr{B}_j(t)$ in terms of monomials:

$$D^{\xi}_{\sigma,\mu,\omega}\mathscr{B}_j(t) = \sum_{i=0}^{j} \binom{j}{i} \mathscr{B}_{j-i}\, D^{\xi}_{\sigma,\mu,\omega} t^i.$$

Next, we apply Theorem 2.11, which gives the regularized Prabhakar fractional derivative of the monomial t^i in the Caputo sense. Noting that this derivative vanishes for $i < \lceil\mu\rceil$, we obtain

$$D^{\xi}_{\sigma,\mu,\omega}\mathscr{B}_j(t) = \sum_{i=\lceil\mu\rceil}^{j} \binom{j}{i} \mathscr{B}_{j-i} \sum_{k=0}^{\infty} \frac{\Gamma(-\xi+k)\,\omega^k\,\Gamma(i+1)\,t^{\sigma k-\mu+i}}{\Gamma(-\xi)\,\Gamma(\sigma k-\mu+i+1)\,\Gamma(k+1)}.$$

To express the result in terms of Bernoulli polynomials, we approximate the monomial $t^{\sigma k-\mu+i}$ by its projection onto the Bernoulli basis, as described in Section 2.2:

$$t^{\sigma k-\mu+i} \approx \sum_{l=0}^{N} g_l^{(k,i)}\, \mathscr{B}_l(t).$$

Substituting this approximation back into the previous expression yields

$$D^{\xi}_{\sigma,\mu,\omega}\mathscr{B}_j(t) \approx \sum_{i=\lceil\mu\rceil}^{j} \binom{j}{i} \mathscr{B}_{j-i} \sum_{k=0}^{\infty} \frac{\Gamma(-\xi+k)\,\omega^k\,\Gamma(i+1)}{\Gamma(-\xi)\,\Gamma(\sigma k-\mu+i+1)\,\Gamma(k+1)} \sum_{l=0}^{N} g_l^{(k,i)}\, \mathscr{B}_l(t).$$

Interchanging the summation order, we obtain

$$D^{\xi}_{\sigma,\mu,\omega}\mathscr{B}_j(t) \approx \sum_{l=0}^{N} \left(\sum_{i=\lceil\mu\rceil}^{j} \binom{j}{i} \mathscr{B}_{j-i} \sum_{k=0}^{\infty} \frac{\Gamma(-\xi+k)\,\omega^k\,\Gamma(i+1)\,g_l^{(k,i)}}{\Gamma(-\xi)\,\Gamma(\sigma k-\mu+i+1)\,\Gamma(k+1)} \right) \mathscr{B}_l(t).$$

This shows that the action of the operator $D^{\xi}_{\sigma,\mu,\omega}$ on the Bernoulli polynomial $\mathscr{B}_j(t)$ can be approximated by a linear combination of Bernoulli polynomials. Therefore, the (j,l)-th entry of the operational matrix $\mathbf{P}^{\xi}_{\sigma,\mu,\omega}$ is given by

$$[\mathbf{P}^{\xi}_{\sigma,\mu,\omega}]_{j,l} = \sum_{i=\lceil\mu\rceil}^{j} \zeta^{\xi}_{j,i,\sigma,\mu,\omega,l},$$

where

$$\zeta^{\xi}_{j,i,\sigma,\mu,\omega,l} = \binom{j}{i} \mathscr{B}_{j-i} \sum_{k=0}^{\infty} \frac{\Gamma(-\xi+k)\,\omega^k\,\Gamma(i+1)\,g_l^{(k,i)}}{\Gamma(-\xi)\,\Gamma(\sigma k-\mu+i+1)\,\Gamma(k+1)}.$$

Finally, for $j < \lceil\mu\rceil$, the fractional derivative vanishes and the corresponding row of the matrix is zero. This completes the proof. □

4. Error Analysis

Lemma 4.1 ([20]). *Let $\mathscr{W} \in C^{N+1}[0,1]$ and let $\mathcal{X}_N$ be the linear space spanned by Bernoulli polynomials up to degree N. If $\mathscr{W}_N(t)$ is the best approximation of $\mathscr{W}$ in the L^2-norm, then*

$$\|\mathscr{W} - \mathscr{W}_N\|_{L^2[0,1]} \leqslant \frac{K}{(N+1)!}\sqrt{\frac{1}{2N+3}}, \qquad \text{where} \qquad K = \sup_{t\in[0,1]} \left|\mathscr{W}^{(N+1)}(t)\right|.$$

Theorem 4.2. *For any function $\mathscr{W} \in L^2[0,1]$ approximated by $\mathscr{W}_N(t) = c^T\mathscr{B}(t)$, we have*

$$\lim_{N\to\infty} \left\|\mathscr{W} - \mathscr{W}_N\right\|_{L^2[0,1]} = 0.$$

Theorem 4.3. *In a Hilbert space $\mathcal{H}$ with finite-dimensional subspace $\mathcal{Y}$ spanned by an orthonormal basis $\{y_1, \ldots, y_n\}$, the best approximation $y_0 \in \mathcal{Y}$ to $x \in \mathcal{H}$ satisfies*

$$\|x - y_0\|_2^2 = \|x\|_2^2 - \sum_{k=1}^{n} \left|\langle x, y_k\rangle\right|^2.$$

Equivalently, using Gram determinants,

$$\|x - y_0\|_2^2 = \frac{G(x, y_1, \ldots, y_n)}{G(y_1, \ldots, y_n)},$$

where G denotes the Gram determinant of the specified set of vectors.

The approximation error for the Prabhakar fractional derivative is bounded by

$$\epsilon_j(t) = D^{\xi}_{\sigma,\mu,\omega}\mathscr{B}_j(t) - \sum_{l=0}^{N}\sum_{i=\lceil\mu\rceil}^{j} \zeta^{\xi}_{j,i,\sigma,\mu,\omega,l}\,\mathscr{B}_l(t).$$

The L^2-norm of this error satisfies

$$\left\|\epsilon_j\right\|_{L^2[0,1]} \leqslant \sum_{i=\lceil\mu\rceil}^{j} \binom{j}{i} \left|\mathscr{B}_{j-i}\right| \sum_{k=0}^{\infty} \left|\Lambda_{k,i}\right| \left\| t^{\sigma k-\mu+i} - \sum_{l=0}^{N} g_l^{(k,i)}\mathscr{B}_l(t)\right\|_{L^2[0,1]},$$

where

$$\Lambda_{k,i} = \frac{\Gamma(-\xi+k)\,\omega^k\,\Gamma(i+1)}{\Gamma(-\xi)\,\Gamma(\sigma k-\mu+i+1)\,\Gamma(k+1)}$$

and $g_l^{(k,i)}$ are the projection coefficients. As $N \to \infty$, each approximation error term vanishes and thus

$$\lim_{N\to\infty} \left\|\epsilon_j\right\|_{L^2[0,1]} = 0.$$

5. The Numerical Method

The general form of the regularized Prabhakar fractional optimal control problems considered in this study is given by

$$\min J = \int_0^1 \left(x^2(t) + u^2(t) + w(t)x(t) + z(t)u(t)\right) dt, \tag{5.1}$$

$$\text{subject to:} \quad {}^{C}\mathbf{D}^{\xi}_{\sigma,\mu,\omega,0^+} x(t) = g\big(t, x(t), u(t)\big), \tag{5.2}$$

$$x(0) = a. \tag{5.3}$$

To solve (5.2)(5.3), we approximate $x(t)$ and $u(t)$ using Bernoulli polynomial expansions:

$$x(t) = X^T \mathscr{B}(t), \tag{5.4}$$
$$u(t) = U^T \mathscr{B}(t), \tag{5.5}$$

where $X = [x_0, x_1, \ldots, x_N]^T$ and $U = [u_0, u_1, \ldots, u_N]^T$ are unknown coefficient vectors, and $\mathscr{B}(t)$ is the Bernoulli basis vector.

Using the operational matrix $P^{\xi}_{\sigma,\mu,\omega}$ for the regularized Prabhakar derivative (Theorem 3.1), we have

$${}^{C}\mathbf{D}^{\xi}_{\sigma,\mu,\omega,0^+} x(t) \approx X^T P^{\xi}_{\sigma,\mu,\omega} \mathscr{B}(t). \tag{5.6}$$

Substituting (5.4), (5.5), and (5.6) into (5.2) yields

$$X^T P^{\xi}_{\sigma,\mu,\omega} \mathscr{B}(t) = g\big(t, X^T \mathscr{B}(t), U^T \mathscr{B}(t)\big). \tag{5.7}$$

We expand the known functions in the Bernoulli series:

$$w(t) = W^T \mathscr{B}(t), \qquad z(t) = Z^T \mathscr{B}(t), \tag{5.8}$$

where W and Z are known coefficient vectors.

The initial condition becomes

$$X^T \mathscr{B}(0) = a. \tag{5.9}$$

The cost functional (5.1) is approximated as

$$J \simeq \int_0^1 \Big(X^T \mathscr{B}(t) \mathscr{B}^T(t) X + U^T \mathscr{B}(t) \mathscr{B}^T(t) U + W^T \mathscr{B}(t) \mathscr{B}^T(t) X + Z^T \mathscr{B}(t) \mathscr{B}^T(t) U \Big)\, dt. \tag{5.10}$$

Then we obtain

$$J[X, U] = X^T H X + U^T H U + W^T H X + Z^T H U, \tag{5.11}$$

where $H \in \mathbb{R}^{(N+1)\times(N+1)}$ is computed according to (2.16). We formulate the constrained optimization problem using Lagrange multipliers $\Lambda = [\lambda_0, \lambda_1, \ldots, \lambda_N]^T$:

$$\mathcal{J} = J[X, U] + \Lambda^T \big(X^T P^{\xi}_{\sigma,\mu,\omega} - G(X, U) \big), \tag{5.12}$$

where $G(X, U)$ encodes the dynamical constraint (5.7).

The optimality conditions are

$$\frac{\partial \mathcal{J}}{\partial X} = 0, \qquad \frac{\partial \mathcal{J}}{\partial U} = 0, \qquad \frac{\partial \mathcal{J}}{\partial \Lambda} = 0. \tag{5.13}$$

Solving this nonlinear algebraic system yields the coefficients X and U, from which we reconstruct $x(t)$ and $u(t)$ via (5.4) and (5.5).

6. Illustrative Examples

To validate the proposed method outlined in Section 5, we apply it to several illustrative numerical examples.

Example 6.1. Consider the following fractional optimal control problem:

$$\min J = \frac{1}{2}\int_0^1 \left(x^2(t) + u^2(t)\right) dt, \tag{6.1}$$

$$\text{subject to:} \quad {}^{C}\mathbf{D}^{\xi}_{\sigma,\mu,\omega,0^+} x(t) + x(t) - u(t) = 0, \tag{6.2}$$

$$x(0) - 1 = 0. \tag{6.3}$$

For the particular case where $\xi = 0$ and $\mu = 1$, the exact solution is given by

$$\begin{aligned} x(t) &= \cosh(\sqrt{2}\,t) + \nu \sinh(\sqrt{2}\,t), \\ u(t) &= (1 + \sqrt{2}\nu)\cosh(\sqrt{2}\,t) + (\sqrt{2} + \nu)\sinh(\sqrt{2}\,t), \\ \nu &= -\frac{\cosh(\sqrt{2})}{\sqrt{2}\,\cosh(\sqrt{2}) + \sinh(\sqrt{2})} + \frac{\sqrt{2}\,\sinh(\sqrt{2})}{\sqrt{2}\,\cosh(\sqrt{2}) + \sinh(\sqrt{2})}. \end{aligned}$$

The corresponding optimal cost is $J^* = 0.192909$.

Following the numerical scheme detailed in Section 5, the solution procedure begins by constructing the regularized Prabhakar operational matrix, approximating the state and control functions using Bernoulli polynomials, and formulating the optimality conditions via Lagrange multipliers. The resulting algebraic system yields the coefficients of the approximate solution.

Table 1: Cost functional error ΔJ for $\sigma = 1, \mu = 1, \xi = 0, \omega = 0.25$ and different polynomial degrees N.

N	2	3	4	5	6
ΔJ	1.387×10^{-3}	2.231×10^{-5}	1.469×10^{-7}	8.171×10^{-10}	4.483×10^{-11}

In Table 1, the cost functional error ΔJ is reported for increasing degrees N of the Bernoulli polynomial basis. The results show clear exponential decay in ΔJ with increasing N, confirming the strong convergence of the proposed numerical method. For instance, the error decreases from 1.387×10^{-3} for $N = 2$ to less than 10^{-10} for $N = 5$, indicating that the approximate solution closely approaches the exact one. This trend confirms the efficiency and high accuracy of the Bernoulli operational matrix approach in approximating the optimal control and the associated cost functional within the framework of the regularized Prabhakar derivative. Figure 1 displays the absolute errors of the approximate state $\tilde{x}(t)$ and control $\tilde{u}(t)$ for various degrees N of the Bernoulli polynomial basis. Each curve corresponds to a distinct value of $N \in \{2, 3, 4, 5, 6\}$.

The graphs clearly show that the errors decrease as N increases, confirming the convergence behavior already observed in Table 1. Notably, the approximation of the control function $u(t)$ shows a slightly slower convergence compared to the state $x(t)$, but both reach high accuracy for $N \geqslant 5$.

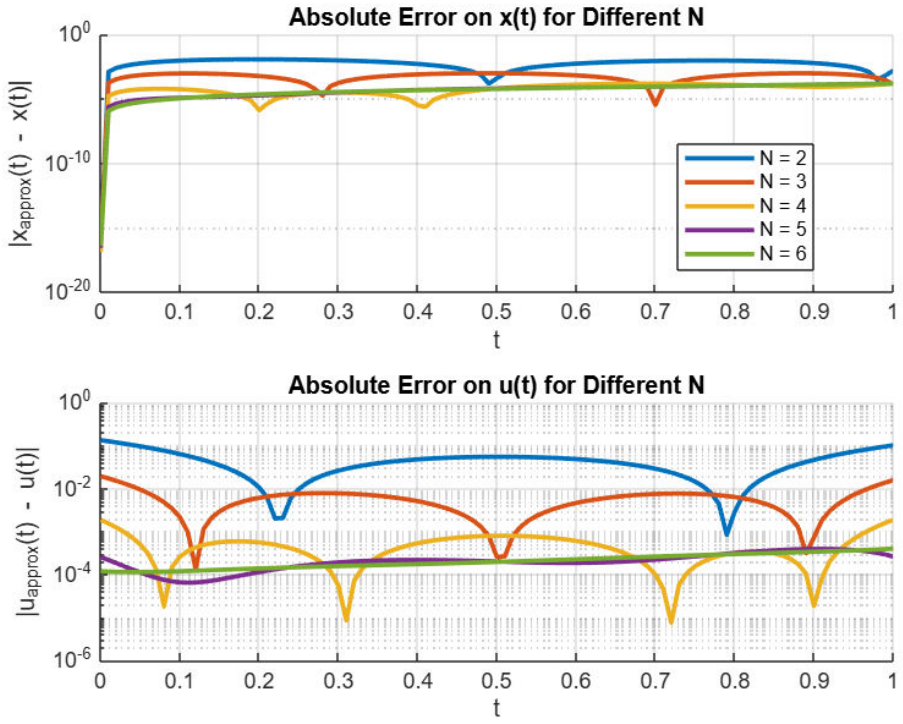

Figure 1: Absolute errors in $x(t)$ and $u(t)$ for $\sigma = 1, \mu = 1, \xi = 0, \omega = 0.25$ and various values of N.

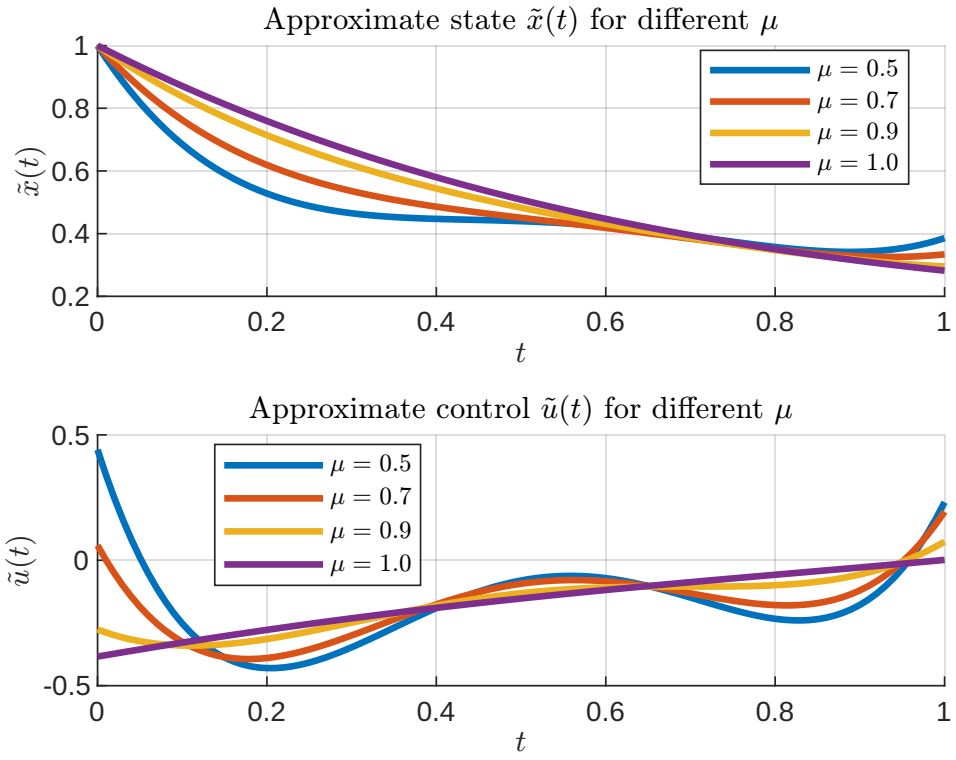

Figure 2: State and control approximations for $\sigma = 1, \xi = 0, \omega = 0.25$ and different fractional orders μ, with $N = 4$.

In Figure 2, the approximate solutions $\tilde{x}(t)$ (top) and $\tilde{u}(t)$ are displayed for $\xi = 0$ and different values of the fractional order $\mu \in \{0.5, 0.7, 0.9, 1\}$, using a Bernoulli polynomial basis of degree $N = 4$. As μ approaches 1, the solutions tend to the classical case.

Table 2: Cost functional for $\sigma = 1, \xi = 0, \omega = 0.25$ and different μ, with $N = 4$.

μ	0.5	0.7	0.9	0.99	1
J	0.1496514212	0.1605231482	0.1799602266	0.1915355806	0.1929094450

Table 2 presents the numerical values of the cost functional J obtained for different values of the parameter μ, with the approximation degree fixed at $N = 4$. It is clearly observed that the value of $J(\mu)$ increases monotonically with μ. This trend reflects the fact that higher values of μ correspond to dynamical regimes where the control $u(t)$ has a stronger or more prolonged influence on the system, thus resulting in a higher associated cost.

Moreover, the variations in J become more significant for $\mu \in [0.9, 1]$, which may indicate a stiffer system behavior as μ approaches the classical integer-order case $\mu = 1$.

Example 6.2. This example studies an optimal control problem involving the regularized Prabhakar fractional derivative in place of the classical derivative. This formulation, inspired by the work of Barikbin and Keshavarz [7], involves minimizing a cost functional subject to a fractional dynamic constraint:

$$\min J = \int_0^1 \left(0.625\, x^2(t) + 0.5\, u^2(t) + 0.5\, x(t)\, u(t)\right) dt. \tag{2.1}$$

subject to

$$D^{\xi}_{\sigma,\mu,\omega,0^+} x(t) - 0.5\, x(t) - u(t) = 0, \tag{2.2}$$

with

$$x(0) - 1 = 0. \tag{6.4}$$

For the special case $\xi = 0$ and $\mu = 1$, the exact solution is known and given by

$$u^*(t) = -\frac{(\tanh(1-t) + 0.5)\, \cosh(1-t)}{\cosh(1)}, \tag{2.3}$$

$$x^*(t) = \frac{\cosh(1-t)}{\cosh(1)}. \tag{2.4}$$

The associated optimal cost is

$$J^* = 0.3807971.$$

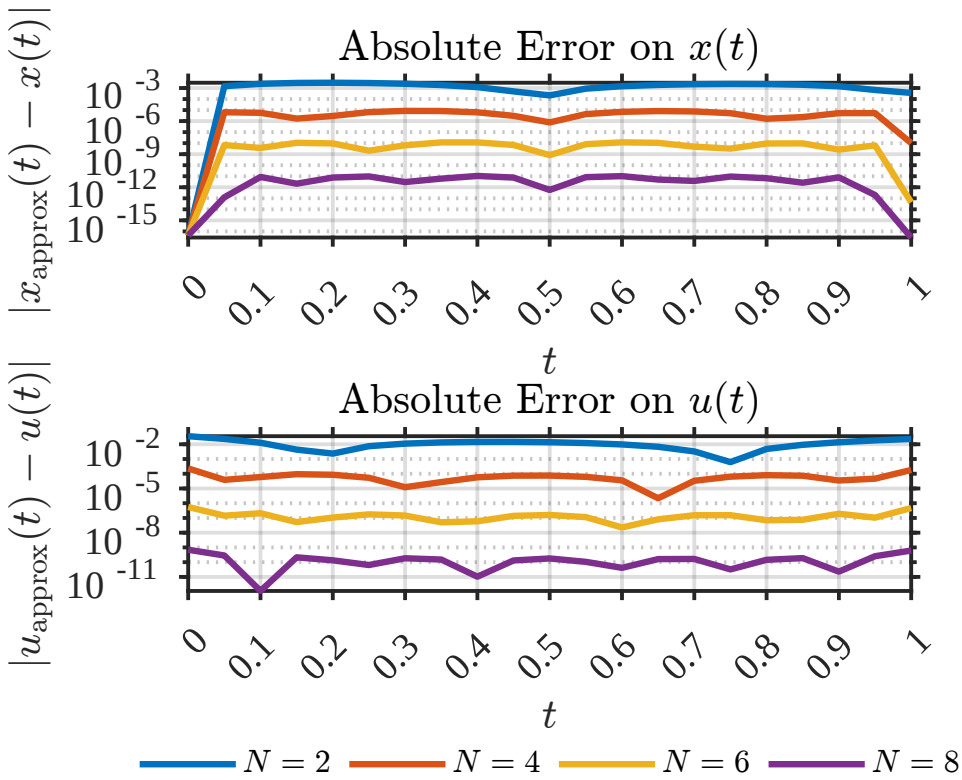

Figure 3: Absolute errors for $x(t)$ and $u(t)$ with $\sigma = 1, \mu = 1, \xi = 0, \omega = 0.25$, and various $N = 2, 4, 6, 8$.

Figure 3 illustrates the evolution of the absolute errors in the state variable $x(t)$ and the control function $u(t)$ as the approximation degree increases ($N = 2, 4, 6, 8$). The graphical results demonstrate a clear, rapid decrease in error magnitude, confirming the convergence and effectiveness of the numerical scheme.

Table 3: Summary of absolute error norms for $x(t)$ and $u(t)$ with $\sigma = 1, \mu = 1, \xi = 0, \omega = 0.25$ at various values of N.

	Errors on $x(t)$		**Errors on** $u(t)$	
N	$L_\infty(x)$	$L_2(x)$	$L_\infty(u)$	$L_2(u)$
2	3.010×10^{-3}	1.915×10^{-3}	3.537×10^{-2}	1.668×10^{-2}
4	8.402×10^{-6}	5.344×10^{-6}	2.291×10^{-4}	1.072×10^{-4}
6	1.185×10^{-8}	7.334×10^{-9}	5.561×10^{-7}	2.648×10^{-7}
8	1.056×10^{-11}	6.897×10^{-12}	6.979×10^{-10}	3.160×10^{-10}

Table 3 quantitatively demonstrates the accuracy and reliability of the developed numerical scheme. As the polynomial degree N increases, the L_∞ and L_2 norms of the absolute errors for both the state variable $x(t)$ and the control function $u(t)$ exhibit a substantial and consistent decrease, often by several orders of magnitude. These results confirm the method's high accuracy, efficiency, and spectral convergence, in agreement with the graphical observations.

Table 4: Cost J^* for each polynomial degree N ($\sigma = 1, \xi = 0, \omega = 0.25$ and $\mu = 1$).

N	4	6	8
J^*	0.3807970803	0.38079707798	0.38079707797788

Table 4 presents the computed optimal values J^* for different values of N. The results converge rapidly to the exact value, demonstrating both the accuracy and numerical stability of the technique.

Table 5: Absolute errors at selected time points for different polynomial degrees $N = 4, 6, 8$, with $\sigma = 1, \xi = 0, \omega = 0.25$ and $\mu = 1$.

Time	$N = 4$		$N = 6$		$N = 8$	
	$\lvert x - x_{exact}\rvert$	$\lvert u - u_{exact}\rvert$	$\lvert x - x_{exact}\rvert$	$\lvert u - u_{exact}\rvert$	$\lvert x - x_{exact}\rvert$	$\lvert u - u_{exact}\rvert$
0.1	5.649×10^{-6}	5.978×10^{-5}	3.664×10^{-9}	2.091×10^{-7}	8.590×10^{-12}	1.113×10^{-12}
0.2	2.915×10^{-6}	8.509×10^{-5}	9.417×10^{-9}	1.063×10^{-7}	7.594×10^{-12}	1.334×10^{-10}
0.3	8.402×10^{-6}	1.224×10^{-5}	6.376×10^{-9}	1.457×10^{-7}	2.959×10^{-12}	1.840×10^{-10}
0.4	6.239×10^{-6}	5.738×10^{-5}	1.174×10^{-8}	5.940×10^{-8}	1.056×10^{-11}	1.039×10^{-11}
0.5	7.623×10^{-7}	7.531×10^{-5}	8.290×10^{-10}	1.590×10^{-7}	5.687×10^{-13}	1.785×10^{-10}
0.6	6.935×10^{-6}	3.585×10^{-5}	1.185×10^{-8}	2.267×10^{-8}	1.019×10^{-11}	4.123×10^{-11}
0.7	7.512×10^{-6}	3.335×10^{-5}	4.791×10^{-9}	1.525×10^{-7}	3.756×10^{-12}	1.649×10^{-10}
0.8	1.642×10^{-6}	7.991×10^{-5}	9.301×10^{-9}	6.949×10^{-8}	6.594×10^{-12}	1.443×10^{-10}
0.9	5.282×10^{-6}	3.480×10^{-5}	2.599×10^{-9}	1.918×10^{-7}	7.894×10^{-12}	2.278×10^{-11}
1.0	9.977×10^{-9}	1.801×10^{-4}	4.366×10^{-14}	4.707×10^{-7}	2.769×10^{-17}	6.145×10^{-10}

Table 6: Cost functional for different μ, with $N = 6$, $\sigma = 1, \xi = 0, \omega = 0.25$.

μ	0.8	0.9	0.99	1
J	0.3524716686	0.366736173	0.3794075	0.380797078

Table 7: Cost functional for different σ, with $N = 6$, $\mu = 1, \xi = 1, \omega = 0.25$.

σ	0.01	0.02	0.1	0.2	1
J	0.38063693	0.380476720	0.379192629	0.3775817051	0.380797078

The influence of the fractional parameters μ, σ, and ξ is investigated in Tables 6 and 7. As $\xi = 0$ and $\mu \to 1$, $\sigma \to 1$, the cost functional J tends toward its reference value obtained in the classical case, highlighting the consistency of the fractional model with integerorder dynamics in the limiting case.

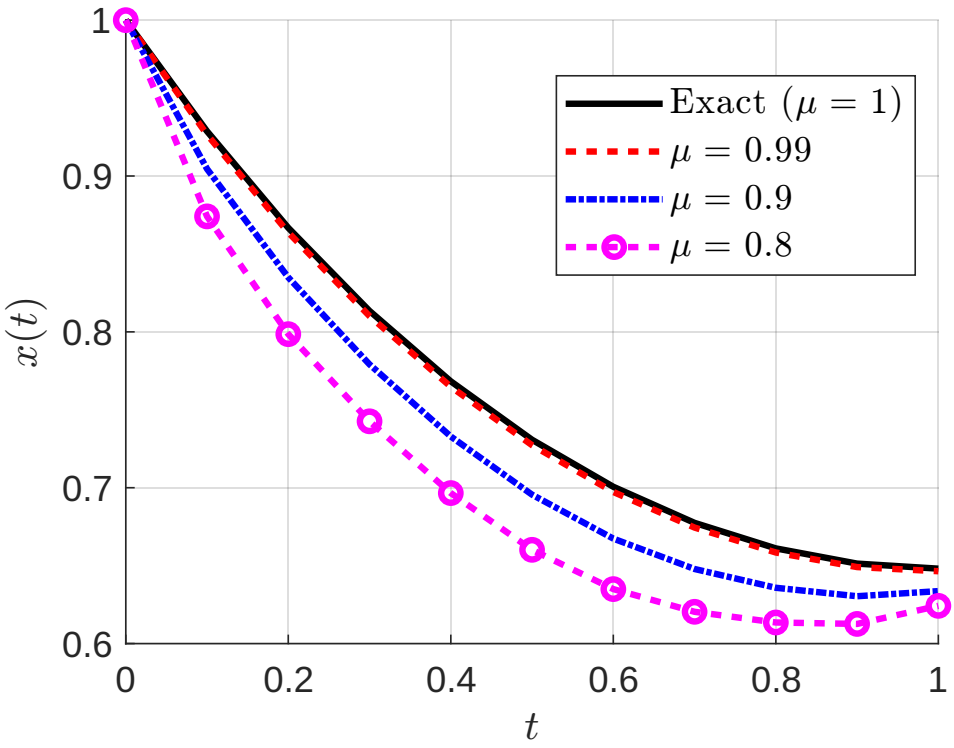

Figure 4: Analysis of approximation accuracy for $x(t)$ with $\xi = 0$ and varying μ.

Figure 4 supports this analysis, showing that smaller values of μ lead to larger deviations from the classical behavior. This reflects the impact of memory effects induced by the regularized Prabhakar operator ${}^{C}\mathcal{D}^{\xi}_{\sigma,\mu,\omega,0^+}$, which generalizes the Caputo derivative by incorporating three fractional parameters.

Example 6.3. Consider the following fractional optimal control problem, as presented in [32]:

$$\min_{x,u} J[x,u] = \frac{1}{2}\int_0^1 \left(3x^2(t) + u^2(t)\right) dt, \tag{6.5}$$

subject to

$${}^{C}\mathbf{D}^{\xi}_{\sigma,\mu,\omega,0^+}x(t) + x(t) - u(t) = 0, \quad 0 \leqslant t \leqslant 1, \tag{6.6}$$

with

$$x(0) = 0, \quad x(1) = 2. \tag{6.7}$$

The exact solution of this problem for $\xi = 0$ and $\mu = 1$ is given by

$$x(t) = 2\frac{\sinh(2t)}{\sinh(2)}, \quad u(t) = 2\sinh(2t) + 2\frac{\cosh(2t)}{\sinh(2)}. \tag{6.8}$$

Table 8: Optimal cost J^* for $\sigma = 1$, $\mu = 1$, $\xi = 0$, $\omega = 0.25$ and different values of N (exact: $J = 6.149258882910192$).

N	6	8	9	10
J^*	6.149258884028549	6.149258882910215	6.149258882910193	6.149258882910193

Table 8 presents the computed optimal cost J^* for various approximation degrees $N = 6, 8, 9, 10$, compared against the exact value $J = 6.149258882910192$. The results demonstrate that the proposed numerical method converges rapidly toward the exact solution as N increases. For $N = 9$ and $N = 10$, the computed values are nearly identical to the exact cost up to machine precision, confirming the method's high accuracy and numerical stability.

Table 9: Absolute errors in $x(t)$ across degrees N for $\sigma = 1$, $\mu = 1$, $\xi = 0$, and $\omega = 0.25$.

t	$N = 6$	$N = 8$	$N = 9$	$N = 10$
0.1	8.96×10^{-7}	1.05×10^{-8}	3.16×10^{-10}	6.68×10^{-12}
0.2	3.08×10^{-7}	8.84×10^{-9}	4.49×10^{-10}	1.25×10^{-11}
0.3	1.63×10^{-6}	4.79×10^{-9}	3.39×10^{-10}	2.74×10^{-11}
0.4	3.87×10^{-6}	1.34×10^{-8}	1.97×10^{-10}	2.58×10^{-11}
0.5	1.91×10^{-7}	5.23×10^{-10}	5.23×10^{-10}	9.82×10^{-13}
0.6	3.85×10^{-6}	1.37×10^{-8}	1.44×10^{-10}	2.71×10^{-11}
0.7	2.00×10^{-6}	4.06×10^{-9}	3.94×10^{-10}	2.74×10^{-11}
0.8	3.11×10^{-6}	9.76×10^{-9}	4.74×10^{-10}	1.17×10^{-11}
0.9	1.14×10^{-6}	1.12×10^{-8}	3.29×10^{-10}	6.12×10^{-12}

Table 9 displays the computed absolute errors for the state variable $x(t)$ at selected time points and for different values of N. A clear trend of decreasing error with increasing N is observed. For $N = 10$, the error is consistently reduced to the order of 10^{-12} or lower, highlighting the method's spectral convergence. Moreover, the error remains well distributed across the domain, including the central point $t = 0.5$, where high precision is maintained.

Table 10: Absolute error of $u(t)$ for different N at $\sigma = 1$, $\mu = 1$, $\xi = 0$, $\omega = 0.25$.

t	$N = 6$	$N = 8$	$N = 9$	$N = 10$
0.0	1.61×10^{-4}	8.29×10^{-7}	3.61×10^{-8}	2.57×10^{-9}
0.1	6.51×10^{-5}	3.26×10^{-8}	6.12×10^{-9}	7.65×10^{-10}
0.2	2.26×10^{-5}	1.94×10^{-7}	6.65×10^{-10}	6.11×10^{-10}
0.3	5.09×10^{-5}	2.17×10^{-7}	7.84×10^{-9}	2.05×10^{-10}
0.4	6.66×10^{-6}	5.69×10^{-8}	8.88×10^{-9}	3.84×10^{-10}
0.5	5.20×10^{-5}	2.33×10^{-7}	1.17×10^{-9}	6.50×10^{-10}
0.6	2.01×10^{-5}	1.09×10^{-8}	9.91×10^{-9}	2.98×10^{-10}
0.7	4.70×10^{-5}	2.40×10^{-7}	6.60×10^{-9}	3.07×10^{-10}
0.8	3.51×10^{-5}	1.71×10^{-7}	2.88×10^{-9}	6.81×10^{-10}
0.9	6.78×10^{-5}	3.55×10^{-9}	8.36×10^{-9}	8.33×10^{-10}
1.0	1.81×10^{-4}	9.07×10^{-7}	4.14×10^{-8}	2.77×10^{-10}

Table 10 provides the absolute errors of the control function $u(t)$ over the interval $[0, 1]$. Similar to the results for $x(t)$, the errors decrease significantly with increasing N. For instance, the maximum error for $N = 6$ is on the order of 10^{-4}, while for $N = 10$ it drops to as low as 10^{-10}. These results demonstrate that the proposed method accurately captures both the state and control trajectories with high fidelity.

Table 11: Effect of ξ on J^* for $N = 6$, $\mu = 1$, $\sigma = 1$, $\omega = 0.25$.

ξ	0.3	0.2	0.1	1.0
J^*	5.9287752	6.0011659	6.07465838	6.149258884028549

Table 11 shows the influence of the fractional parameter ξ on the optimal cost J^* for a fixed approximation degree $N = 6$. As ξ increases, the optimal cost J^* gradually increases, reaching its maximum when $\xi = 1$. These results underline the importance of carefully tuning ξ in fractional optimal control problems.

Figure 5 illustrates the evolution of the absolute error of the state function $x(t)$ for different approximation degrees $N = 7, 8, 9, 10$, with the parameters fixed at $\mu = 1$, $\sigma = 1$, $\xi = 0$, and $\omega = 0.25$. A clear decrease in the maximum error is observed as N increases. More specifically, the accuracy improves by

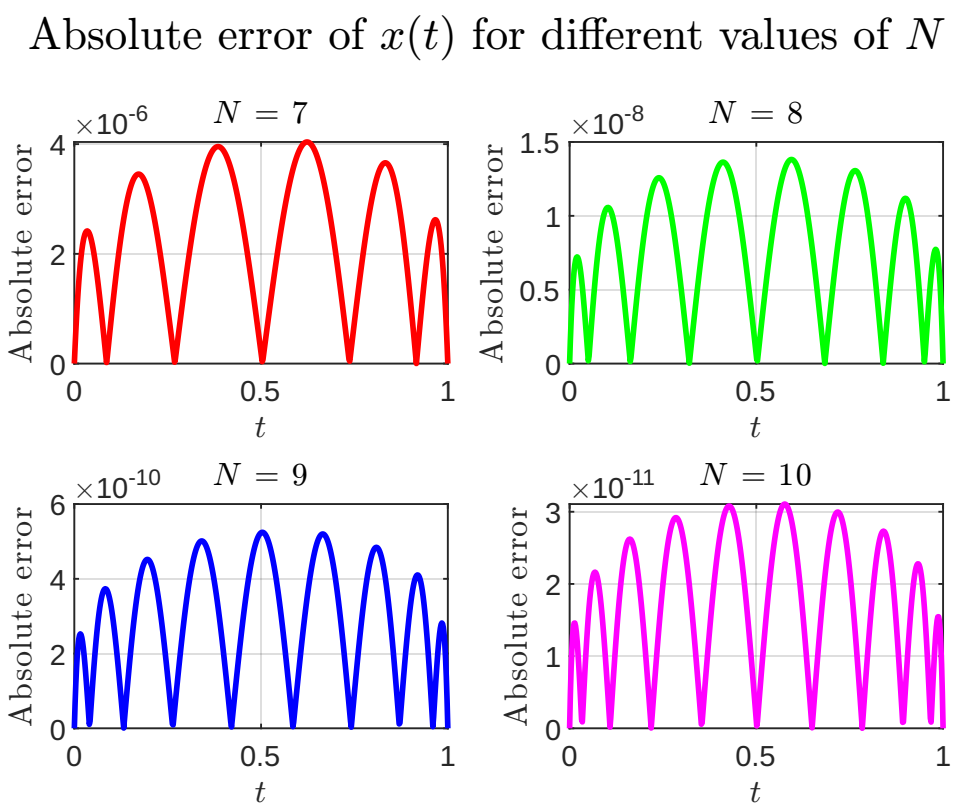

Figure 5: Absolute error of $x(t)$ for $\sigma = 1$, $\mu = 1$, $\xi = 0$, $\omega = 0.25$, and different values $N = 7, 8, 9, 10$.

approximately one order of magnitude with each increment of N, indicating a rapid convergence of the proposed method.

Example 6.4. Consider the following fractional optimal control problem:

$$J(x,u) = \frac{1}{2}\int_0^1 \left(x_1^2(t) + x_2^2(t) + u^2(t)\right) dt,$$

subject to

$$D^{\xi}_{\sigma,\mu,\omega,0^+} x_1(t) = -x_1(t) + x_2(t) + u(t),$$
$$D^{\xi}_{\sigma,\mu,\omega,0^+} x_2(t) = -2x_2(t),$$

with the initial conditions

$$x_1(0) = 1, \quad x_2(0) = 1.$$

The optimal value of the cost functional is approximately $J^* \approx 0.4319835548817479$.

The table below presents the computed cost values J^* for $\xi = 0$, $\mu = 1$ and different approximation degrees N:

N = 5	**N = 7**	**N = 9**	**N = 10**
0.432332	0.4319598	0.431996	0.43199338277

The following table displays the numerical values of $x_1(t)$, $x_2(t)$, and $u(t)$ for various time points $t \in [0, 1]$,

using approximation degree $N = 10$:

t	$x_1(t)$	$x_2(t)$	$u(t)$
0.1	1.3226×10^{-4}	1.5615×10^{-6}	8.63993×10^{-5}
0.2	1.7742×10^{-4}	2.2316×10^{-6}	4.1975×10^{-4}
0.3	1.7743×10^{-4}	1.8082×10^{-6}	1.330848×10^{-4}
0.4	9.7656×10^{-5}	4.9833×10^{-7}	1.26691×10^{-3}
0.5	1.0428×10^{-4}	1.1618×10^{-6}	2.773×10^{-3}
0.6	4.2082×10^{-4}	2.5103×10^{-6}	3.9405×10^{-3}
0.7	7.6343×10^{-4}	3.0094×10^{-6}	3.8118×10^{-3}
0.8	9.5991×10^{-4}	2.4480×10^{-6}	1.4502×10^{-3}
0.9	7.7539×10^{-4}	1.0231×10^{-6}	3.8458×10^{-3}

It is observed that the functional value J^* rapidly converges to the exact optimal value as the approximation degree N increases. Additionally, the values of the state and control functions $x_1(t)$, $x_2(t)$, and $u(t)$ remain very small across the interval, indicating effective stabilization of the system by the control strategy.

7. Conclusion

In this study, we first constructed the operational matrix of Bernoulli polynomials associated with the regularized Prabhakar derivative. This matrix, in combination with the product matrix, was employed to convert the original optimization problem into a finite-dimensional one, which can be efficiently solved using the Lagrange multiplier method or dedicated numerical solvers. Through this process, the integro-differential problem was transformed into an equivalent algebraic problem.

The numerical results clearly demonstrate that the approximate solution converges to the exact analytical solution as the number of Bernoulli polynomials increases, confirming the efficiency and reliability of the proposed method. Moreover, the numerical experiments indicate that as the parameter ξ tends to zero, the approximate control and state functions converge to those corresponding to the Caputo derivative. Similarly, when the parameter μ approaches one, the solutions converge to those of the classical (ordinary) derivative case.

Future work will focus on extending the use of this operational matrix to design efficient numerical schemes for general classes of optimal control problems and differential equations involving the Prabhakar derivative. Additionally, we plan to develop operational matrices for other families of functions and polynomials to broaden the applicability of the proposed approach to a wider range of related problems.

References

[1] Agrawal, O. (2004). A general formulation and solution scheme for fractional optimal control problems. Nonlinear Dyn, 38, 323337. 1

[2] Agrawal, O. P., and Baleanu, D. (2007). A Hamiltonian formulation and a direct numerical scheme for fractional optimal control problems. J. Vib. Control, 13(9–10), 1269–1281. 1

[3] Agrawal, O. P. (2008). A quadratic numerical scheme for fractional optimal control problems. J. Dyn. Sys. Meas. Control, 130(1), 011010. 1

[4] Agrawal, O. P. (2008). A formulation and numerical scheme for fractional optimal control problems. Journal of Vibration and Control, 14(9–10), 1291–1299. 1

[5] Anderson, B. D. O., and Moore, J. B. (2007). Optimal control: Linear quadratic methods. Dover Publications. 1

[6] Bagley, R. L., and Torvik, P. J. (1983). A theoretical basis for the application of fractional calculus to viscoelasticity. J. Rheol., 27, 201–210. 1

[7] Barikbin, Z., and Keshavarz, E. (2020). Solving fractional optimal control problems by new Bernoulli wavelets operational matrices. Optimal Control Applications and Methods, 41(4), 11881210. 6.2

[8] Belgacem, R., Bokhari, A., Kumar, S., Baleanu, D., and Djilali, S. (2022). Projectile motion using three-parameter MittagLeffler function calculus. Mathematics and Computers in Simulation, 195, 2230. 2.2

[9] Bokhari, A., Baleanu, D., and Belgacem, R. (2022). Regularized Prabhakar derivative for partial differential equations. Computational Methods for Differential Equations, 10(3), 726–737. 2
[10] Bokhari, A., Baleanu, D., and Belgacem, R. (2019). Application of Shehu transform to AtanganaBaleanu derivatives. J. Math. Comput. Sci., 20, 101–107. 2.3
[11] Bokhari, A., Amir, A., Bahri, S. M., and Belgacem, F. B. (2017). A generalized Bernoulli wavelet operational matrix of derivative applications to optimal control problems. Nonlinear Studies, 24(4), 775–790. 1
[12] Bryson, A. E., and Ho, Y.-C. (1975). Applied optimal control: Optimization, estimation, and control. Taylor and Francis. 1
[13] Noori Dalawi, A., Lakestani, M., and Ashpazzadeh, E. (2023). Solving fractional optimal control problems involving CaputoFabrizio derivative using Hermite spline functions. Iran. J. Sci., 47, 545–566. 1
[14] Duckenfield, M. J. (1975). Linear optimal control systems. Review of: Kwakernaak, H. and Sivan, R., WileyInterscience, Chichester, 1972. The Aeronautical Journal, 79(773), 230. 1
[15] Erdélyi, A., Magnus, W., Oberhettinger, F., and Tricomi, F. G. (1955). Higher Transcendental Functions, Vol. 3. McGrawHill, New York. 2.3
[16] Garra, R., Gorenflo, R., Polito, F., and Tomovski, Z. (2014). HilferPrabhakar derivatives and some applications. Applied Mathematics and Computation, 242, 57–589. 2.7
[17] Giusti, A., Colombaro, I., Garra, R., et al. (2020). A practical guide to Prabhakar fractional calculus. Fract. Calc. Appl. Anal., 23, 954. 2, 2.8
[18] Ionescu, C., Lopes, A., Copot, D., Machado, J. A. T., and Bates, J. H. T. (2017). The role of fractional calculus in modeling biological phenomena: A review. Communications in Nonlinear Science and Numerical Simulation, 51, 141–159. 1
[19] Kilbas, A. A., Saigo, M., and Saxena, R. K. (2004). Generalized MittagLeffler function and generalized fractional calculus operators. Integral Transforms and Special Functions, 15(1), 31–49. 2.5
[20] Keshavarz, E., Ordokhani, Y., and Razzaghi, M. (2015). A numerical solution for fractional optimal control problems via Bernoulli polynomials. Journal of Vibration and Control, 22(18), 3889–3903. 1, 4.1
[21] Suhak, L., Youngki, K., Jason, B., Siegel, A. G., and Stefanopoulou, A. G. (2021). Optimal control for fast acquisition of equilibrium voltage for Li-ion batteries. Journal of Energy Storage, 40, 102814. 1
[22] Lewis, F. L., Dawson, D. M., and Abdallah, C. T. (2004). Robot Manipulator Control: Theory and Practice, 2nd ed., revised and expanded. CRC Press. 1
[23] Lotfi, A., Yousefi, S. A., and Dehghan, M. (2013). Numerical solution of a class of fractional optimal control problems via the Legendre orthonormal basis combined with the operational matrix and the Gauss quadrature rule. J. Comput. Appl. Math., 250, 143–160. 1
[24] Magin, R. L. (2004). Fractional calculus in bioengineering, Part 2. Crit. Rev. Biomed. Eng., 32, 105–193. 1
[25] Mainardi, F. (1997). Fractional calculus: Some basic problems in continuum and statistical mechanics. In *Fractals and Fractional Calculus in Continuum Mechanics*. 1
[26] Mophou, G. M. (2011). Optimal control of fractional diffusion equation. Comput. Math. Appl., 61(1), 68–78. 1
[27] Mophou, G. M., and N'Guérékata, G. M. (2011). Optimal control of a fractional diffusion equation with state constraints. Comput. Math. Appl., 62(3), 1413–1426. 1
[28] Nasrudin, F. S. Md., and Phang, C. (2022). Numerical solution via operational matrix for solving Prabhakar fractional differential equations. Journal of Mathematics, 2022, Article ID 7220433. 2.10
[29] Nezhadhosein, S., Ghanbari, R., and Ghorbani-Moghadam, K. (2022). A numerical solution for fractional linear quadratic optimal control problems via shifted Legendre polynomials. Int. J. Appl. Comput. Math., 8, 158. 1
[30] Polito, F., and Tomovski, . (2016). Some properties of Prabhakar-type fractional calculus operators. Fractional Calculus and Applied Analysis, 19(1), 212232. 2.9
[31] Prabhakar, T. R. (1971). A singular integral equation with a generalized MittagLeffler function in the kernel. Yokohama Mathematical Journal, 19, 715. 2.3, 2.4, 2.6
[32] Rabiei, K., Ordokhani, Y., and Babolian, E. (2017). The Boubaker polynomials and their application to solve fractional optimal control problems. Nonlinear Dyn., 88, 1013–1026. 1, 6.3
[33] Rabiei, K., and Ordokhani, Y. (2020). A new operational matrix based on Boubaker wavelet for solving optimal control problems of arbitrary order. Transactions of the Institute of Measurement and Control, 42(10), 1858–1870. 1
[34] Rahimkhani, P., Ordokhani, Y., and Babolian, E. (2016). An efficient approximate method for solving delay fractional optimal control problems. Nonlinear Dyn., 86(3), 1649–1661. 1
[35] Razzaghi, M., and Yousefi, S. (2002). Legendre wavelets method for constrained optimal control problems. Math. Methods Appl. Sci., 25, 529–539. 1
[36] Rosewater, D. M., Copp, D. A., Nguyen, T. A., Byrne, R. H., and Santoso, S. (2019). Battery energy storage models for optimal control. IEEE Access, 7, 178357–178391. 1
[37] Samko, S. G., Kilbas, A. A., and Marichev, O. I. (1993). Fractional Integrals and Derivatives Theory and Applications. Gordon and Breach Science Publishers. 2.1
[38] Shabani, Z., and Tajadodi, H. (2019). A numerical scheme for constrained optimal control problems. International Journal of Industrial Electronics, Control and Optimization, 2(3), 233238. 1
[39] Tajadodi, H. (2020). Efficient technique for solving variable order fractional optimal control problems. Alexandria

Engineering Journal, 59(6), 51795185. 1

[40] Tajadodi, H., Jafari, H., and Ncube, M. N. (2022). Genocchi polynomials as a tool for solving a class of fractional optimal control problems. IJOCTA, 12(2), 160–168. 1

[41] Tajadodi, H., Khan, A., Gomez-Aguilar, J. F., and Khan, H. (2020). Optimal control problems with Atangana-Baleanu fractional derivative. Optim. Control Appl. Methods, 42(1), 96–109. 1

[42] Weber, T. A., and Kryazhimskiy, A. V. (2019). Optimal Control Theory with Applications in Economics. MIT Press. 1

[43] Wiman, A. (1905). Über den Fundamentalsatz in der Theorie der Funktionen $E_\sigma(x)$. Acta Math., 29(1), 191–201. 2.3

[44] Yıldız, T. A., Jajarmi, A., Yldz, B., and Baleanu, D. (2020). New aspects of time fractional optimal control problems within operators with nonsingular kernel. Discrete and Continuous Dynamical Systems S, 13(3), 407–428. 1